JOURNAL OF SPACECRAFT AND ROCKETS
Vol. 43, No. 4, July–August 2006

Preliminary Design of Multiple Gravity-Assist Trajectories

M. Vasile*
Politecnico di Milano, 20156 Milan, Italy
and
P. De Pascale†
University of Padova, 35131 Padua, Italy

The preliminary design of multiple gravity-assist trajectories is formulated as a global optimization problem. An analysis of the structure of the solution space reveals a strong multimodality, which is strictly dependent on the complexity of the model. On the other hand, it is shown how an oversimplification could prevent finding potentially interesting solutions. A trajectory model, which represents a compromise between model completeness and optimization problem complexity, is then presented. The exploration of the resulting solution space is performed through a novel global search approach, which hybridizes an evolutionary-based algorithm with a systematic branching strategy. This approach allows an efficient exploration of complex solution domains by automatically balancing local convergence and global search. A number of difficult multiple gravity-assist trajectory design cases demonstrates the effectiveness of the proposed methodology.

Nomenclature

D_l	=	lth subdomain
F	=	generic objective function
f	=	fitness value
h_k	=	pericenter altitude, km
k	=	phase identification index
L_b	=	lower bound on the design parameters
N_p	=	number of planets of a sequence
$\boldsymbol{n}_\Pi$	=	vector normal to the plane of the hyperbola
p_k	=	planet identification number
$\boldsymbol{q}$	=	quaternion
R	=	residual on the constraint
$\boldsymbol{r}$	=	heliocentric position in Cartesian coordinates, km
S	=	individual exploration region
T	=	time of flight, day
t_{ds}	=	time of deep space maneuver, days
t_0	=	launch date, modified Julian date 2000
U_b	=	upper bound on the design parameters
$\boldsymbol{u}_i$	=	Euler vector for the rotation of the incoming velocity
$\tilde{\boldsymbol{v}}_i$	=	flyby incoming relative velocity, km/s
$\tilde{\boldsymbol{v}}_o$	=	flyby outgoing relative velocity, km/s
v^∞	=	hyperbolic excess velocity, km/s
$\boldsymbol{y}$	=	solution vector
α	=	right ascension of the launch asymptote, rad
γ	=	deflection angle, rad
Δv	=	change of velocity, km/s
δ	=	declination of the launch asymptote, rad
ε	=	epoch of a deep space maneuver as a percentage of transfer time
η_i	=	plane rotation angle, rad
ρ	=	migration radius
σ	=	weighting factor
φ_{Dq}	=	subdomain fitness
ψ_{Dq}	=	subdomain qualification index
ω_{Dq}	=	subdomain density

Received 28 April 2005; revision received 29 July 2005; accepted for publication 3 August 2005.

*Assistant Professor, Department of Aerospace Engineering, Via La Masa 34. Member AIAA.

†Ph.D. Candidate, Centro Interdipartimentale Studi ed Attività Spaziali, Via Venezia 15. Member AIAA.

I. Introduction

THE access to high Δv targets in the solar system has been made possible by the enabling concept of gravity assist,[1,2] through which many missions with challenging objectives were successfully accomplished with significant reductions in launch energy and in transfer time. Past missions, such as Mariner (Ref. 3) 10, Voyager (Ref. 4) 1 and 2, Pioneer 10 and 11, and more recent missions such as Galileo,[5] Ulysses, and Cassini[6] made extensive use of gravity-assist maneuvers; future missions to completely or partially unexplored planets, such as Mercury[7,8] or Pluto,[9,10] will be possible thanks to gravity-assist maneuvers.

The availability of new propulsion systems, such as low-thrust engines, although widening the possibility of flights in the solar system, has not diminished the importance of gravity-assist maneuvers. This is true at least for two different reasons: Many missions will still resort to pure ballistic trajectories using only impulsive corrections and optimal gravity-assist sequences are important in the design of low-thrust gravity-assist trajectories.[7]

Multiple gravity-assist trajectories have been extensively investigated over the past 40 years, and their preliminary design has been approached mainly relying on the experience of mission analysts and following simplifying assumptions in unison with systematic searches or some simple analysis tools such as the Tisserand's graph (see Refs. 1 and 10). This graphical tool, however, turns out to be unsuitable for the investigation of transfers to asteroids and comets with highly eccentric or inclined orbits and for the analysis of transfer options that require additional corrective maneuvers, performed by either high-thrust or low-thrust engines.

On the other hand, because at the early stage of the design of a space mission a number of different options is generally required, it would be desirable to generate automatically many optimal or nearly optimal solutions over the range of the design parameters (escape velocity, launch date, time of flight, etc.) accurately enough to allow a correct tradeoff analysis. This could translate into the need for an exhaustive characterization of highly complex solution domains deriving from sophisticated trajectory models.

Recently, different attempts have been made toward the definition of automatic design tools, although so far most of these tools have been based on systematic search engines. An example is represented by the automatic tool for the investigation of multiple gravity-assist transfers, called STOUR, originally developed by the Jet Propulsion Laboratory[5] and subsequently enhanced at Purdue University.[11–14] This tool has been extensively used for the preliminary investigation of interplanetary trajectories to Jupiter and Pluto,[11,12] for the design of the tour of Jovian moons,[15] and for Earth–Mars cycling trajectories.[16]

Note that such a systematic search methodology, although theoretically complete, could require long computational times, to identify all of the suitable options. Although completeness is a desirable property of any strategy that aims at finding all optimal or suboptimal options, it is also true that this property could remain merely theoretical if the complexity of the problem makes it practically intractable by means of a systematic approach [nondeterministic polynominal time hard (NP-hard) problems].

In the last 10 years, different forms of stochastic search methods have also been applied to orbit design, starting from the work of Hartmann et al.[17] on the use of multiobjective genetic algorithms for the generation of first guess solutions for low-thrust trajectories, to more recent works on the use of single-objective genetic algorithms for ballistic transfers[18] or to the use of hybrid evolutionary search methods for preliminary design of weak stability boundaries and interplanetary transfers.[19,20]

In this paper, we investigate the possibility of using stochastic-based methods for the solution of multiple gravity-assist trajectories and we propose a novel approach for the preliminary automatic design of complex trajectories. First, an analysis of the relation between model and problem complexity will be presented. This will highlight how the structure of the solution space is strongly dependent on the mathematical modeling of gravity-assist maneuvers and transfer trajectories. In particular, it will be shown that problem complexity grows significantly if deep space maneuvers are included and physical constraints on gravity maneuvers are satisfied. On the other hand, models with no deep space maneuvers but with Δv matching at the swing-by planet have a simpler structure,[21] and the related optimization problem can be efficiently solved with a clever systematic search[22] (enumerative, multigrid, or branch and prune). This is even truer if the Δv matching can be performed with an aerogravity maneuver instead of a propelled maneuver.[23]

To handle the complex structure of more realistic models, the use of a novel global search algorithm based on a hybridization of an evolutionary-based search and a deterministic branching strategy[19,20] is proposed. An important feature of this approach is that it combines a stochastic-based search with a complete deterministic decomposition of the solution space. This allows a loose specification of the bounds on the initial solution domain and a parallel exploration of different promising areas of the search space. The output is, therefore, an exhaustive characterization of the search space and a number of alternative families of solutions.

This hybrid approach is here applied to the solution of a number of complex interplanetary transfers both to planets and to comets and asteroids, showing its effectiveness and providing some new solutions to known mission analysis problems.

II. Trajectory Model Analysis

An engineering design problem can always be tackled with a two-stage approach, problem modeling and problem solution, in which often the search for a solution is represented by an optimization procedure. Modeling is the task of transcribing a physical phenomenon into a mathematical representation. The modeling stage has a particular influence on the definition and development of preliminary design methodologies because there is always a tradeoff between the precision of the required solution and the computational cost associated to its search[20]: Different models intrinsically contain different kinds of solutions and can favor or not favor their identification.

This issue takes on significant importance when a large number of good first-guess solutions has to be efficiently generated for an exhaustive preliminary assessment of complex engineering problems. In this case, efficiency is quantified as the ratio between the number of useful solutions and associated computational time. These considerations obviously also apply to trajectory design. Therefore, the two mentioned stages, which are in fact mutually dependent, must be properly defined during the development of an effective design tool for the preliminary investigation of complex interplanetary transfers.

In particular, the modeling process requires the identification of the most important features of the trajectory that will be analyzed and must reproduce the completeness of the problem under investigation, while reducing its complexity. This is a trivial consideration that has nontrivial consequences on the effectiveness of the design phase, because an oversimplified model could lead to the loss of interesting solutions.

On the other hand, a proper mathematical model, which accurately reproduces a physical phenomenon, is likely to require more efficient search methods, to find a specific solution. Therefore, the problem solution stage needs proper search mechanisms or approaches that allow the identification of all relevant solutions in a given solution domain. This raises to the additional issue of the completeness of the search: If the problem is at least NP-hard, a complete search may not be practically possible because the number of function evaluations to prove the optimality of a solution could grow exponentially with problem dimension.

In the following sections, the attention will be focused on some simple trajectory models of increasing complexity to derive a good compromise between computational cost and solution accuracy. When the typical multiple gravity-assist trajectories that have been designed and flown so far are considered, some general features can be considered relevant to maintain the required richness of the search space and to identify all of the families of solutions that could be potentially interesting for the design of an interplanetary mission. In particular, a full three-dimensional model both for the trajectory and for the gravity-assist maneuvers has been developed including deep-space maneuvers (DSMs) and using the analytical ephemeris of celestial bodies. The benefits of such a modeling approach can be seen in the design of missions to Pluto, Mercury, or the sun, which require consideration of the real inclination of the orbit of the planet or of the final heliocentric orbit, and in the design of missions to near-Earth objects. This particular choice is compared, in terms of search space complexity, to a simpler model in which DSMs are neglected. This simple modification prevents consideration of some classes of interesting solutions such as resonant or almost resonant swing-by or free orbits before the encounter with a celestial body.

Because the physics of the solar system allows us the adoption of a patched-conic approximation of a multiple gravity-assist trajectory, a complete transfer trajectory can be reduced to the sum of a number of smaller subproblems with a finite number of design variables. As will be shown in the following sections, each subproblem may produce complex search domains, typically nonconvex and multimodal.

A. Two- and Three-Impulse Transfers

A simple two-impulse direct transfer from planet P_1 to planet P_2 can be modeled as a function of the departure date t_0 and of the arrival date, expressed as the sum of the departure date and of the time of flight T. The two required impulsive maneuvers at departure $\Delta \boldsymbol{v}_1$ and at arrival $\Delta \boldsymbol{v}_2$ can be computed solving Lambert's problem[2] from P_1 to P_2 in a given time T.

An extension of this simple two-impulse model can be obtained by propagating analytically the initial state, given by the position of P_1 and by its velocity plus $\Delta \boldsymbol{v}_1$, for a time $t_{ds} = \varepsilon T$, up to a point M_1 and then by solving Lambert's problem from M_1 to P_2 as in Fig. 1. The resulting discontinuity $\Delta \boldsymbol{v}_s$ in the velocity at M_1 represents a DSM or a correction on the direct transfer. The total cost of the

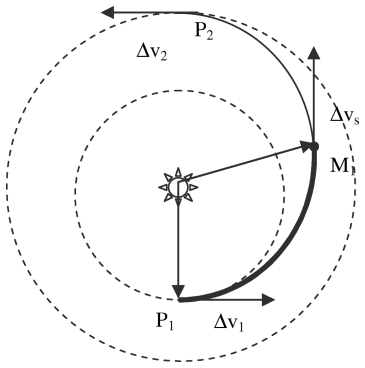

Fig. 1 Schematic of three-impulse transfer.

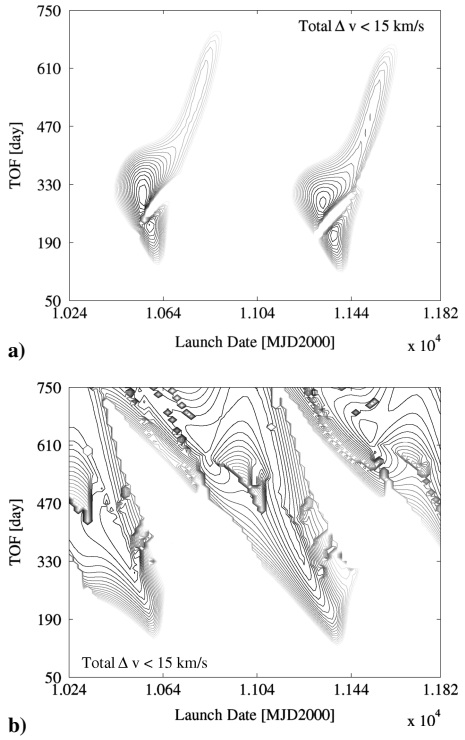

Fig. 2 Solution space for a) two-impulse transfer and b) three-impulse transfer.

transfer can be expressed as

$$f(t_0, \varepsilon, T) = \Delta v_1 + \Delta v_s + \Delta v_2 \tag{1}$$

The structure of the solution space for a two-impulse transfer is directly related to the synodic period of the two bodies P_1 and P_2 and to the orbital elements of their respective orbits, as can be seen in Fig. 2a, where all solutions for a direct Earth–Mars transfer with a total Δv lower than 15 km/s are shown. On the other hand, a DSM increases the number of feasible paths from P_1 to P_2, as can be seen in Fig. 2b, where the function in Eq. (1) has been plotted for all of the optimal values of ε, keeping the Δv at departure aligned along the velocity of the Earth.

B. Gravity-Assist Maneuvers

Gravity-assist (GA) maneuvers are here modeled in three dimensions using a linked-conic approximation: the maneuver is instantaneous, and the sphere of influence is collapsed into a single point. Other two conditions define the physical properties of the gravity maneuver: the incoming and outgoing relative velocities $\tilde{v}_i$ and $\tilde{v}_o$ must have equal modulus and the deflection angle is a function of the pericenter altitude h and of the incoming relative velocity. These conditions typically translate into the following set of constraint equations on position and velocity:

$$\boldsymbol{r}_i = \boldsymbol{r}_o = \boldsymbol{r}_p \tag{2}$$

$$\tilde{v}_i = \tilde{v}_o \tag{3}$$

$$\tilde{\boldsymbol{v}}_o^T \tilde{\boldsymbol{v}}_i = -\cos[2\beta(h)]\tilde{v}_i^2 \tag{4}$$

The constraints on the incoming and outgoing position vectors $\boldsymbol{r}_i$ and $\boldsymbol{r}_o$ and on the planet position vector $\boldsymbol{r}_p$ in Eq. (2), can be explicitly solved, whereas the two conditions in Eqs. (3) and (4) on the relative velocities would require the solution of a constraint satisfaction problem. To avoid the introduction of these nonlinear constraints on GA maneuvers, a different model is used here. By the introduction of an auxiliary rotation angle η it is possible to define the plane of the hyperbola where the rotation of the relative velocity occurs. This is necessary because in the linked-conic approximation the point where the interplanetary trajectories pierces the sphere of influence is not defined and, thus, the plane where the planetocentric hyperbolic motion occurs remains undetermined. This auxiliary angle represents the rotation of a general plane Π, defined through its normal vector $\boldsymbol{n}_\Pi$, round the Euler vector $\boldsymbol{u}_i = \tilde{\boldsymbol{v}}_i / \tilde{v}_i$. Now the vector $\boldsymbol{u}_i$ and the rotation η can be used to define the quaternions:

$$\boldsymbol{q}_\eta = [\boldsymbol{u}_i \sin\eta, \cos\eta]^T \tag{5}$$

Then, any rotation around $\tilde{\boldsymbol{v}}_i$ of a general vector $\boldsymbol{n}_i$ normal to $\tilde{\boldsymbol{v}}_i$ can be expressed as

$$\boldsymbol{n}_\Pi = \boldsymbol{Q}_\eta(\boldsymbol{u}_i)\boldsymbol{n}_i \tag{6}$$

where $\boldsymbol{Q}_\eta$ is a rotation matrix defined by the quaternion $\boldsymbol{q}_\eta$. The normal vector $\boldsymbol{n}_\Pi$ completely defines the orbit plane of the swing-by hyperbola and can be used to define the rotation of the incoming relative vector onto the outgoing relative vector:

$$\tilde{\boldsymbol{v}}_o = \boldsymbol{Q}(\boldsymbol{n}_\Pi)\tilde{\boldsymbol{v}}_i \tag{7}$$

where $\boldsymbol{Q}(\boldsymbol{n}_\Pi)$ is the rotation matrix defined by the quaternion $\boldsymbol{q}_\gamma = [\boldsymbol{n}_\Pi \sin\gamma, \cos\gamma]^T$, with $\gamma = \pi - 2\beta$.

There are different possible choices for the vector $\boldsymbol{n}_i$, depending on which reference plane is adopted. A possible choice is to take this vector as the normal direction to the incoming velocity vector in the xy plane as shown in Fig. 3a. An alternative form could be to define this vector as the normal direction to the plane containing the relative incoming velocity and the planet's velocity $\boldsymbol{V}_p$ as shown in Fig. 3b.

Now, because a maneuver may be necessary to correct the post-swing-by conditions, each GA maneuver can be associated to the following subproblem: Minimize the corrective DSM following the swing-by as a function of the swing-by characteristics and of the trajectory leg before the swing-by. The cost function of this subproblem can be expressed as

$$f(\boldsymbol{v}_i, t_i, h, \eta, \varepsilon, T) = \Delta v_s \tag{8}$$

If the incoming conditions $\boldsymbol{v}_i$, the swing-by epoch t_i, and the post-swing-by transfer time T are kept fixed, then f can be plotted as a function of the angle η and of the altitude of the swing-by h, for different values of parameter ε. Figure 4 show how the solution space progressively changes as the time of the DSM after the

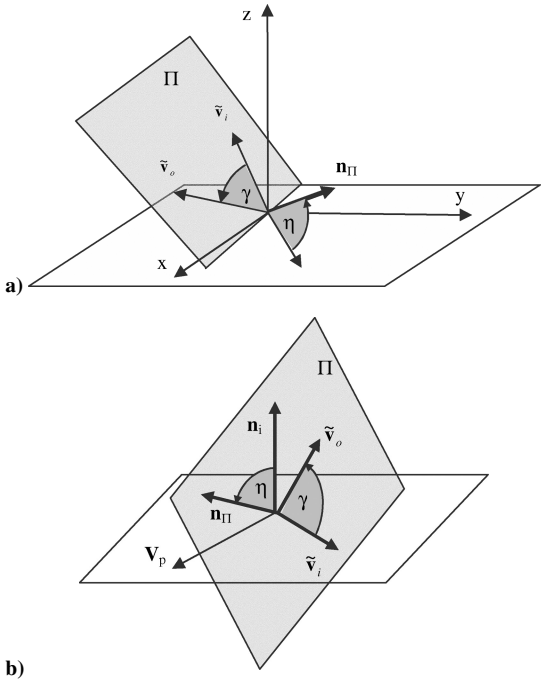

Fig. 3 Schematic of linked-conic model for GA: a) reference direction normal to incoming velocity in *xy* plane and b) reference direction normal to relative and planet's velocity plane.

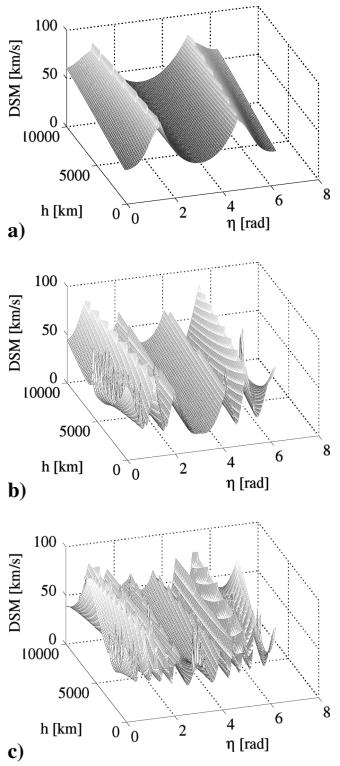

Fig. 4 DSM cost after swing-by for a) impulsive maneuver at 10% of transfer time, b) impulsive maneuver at 37% transfer time, and c) impulsive maneuver at 70% transfer time.

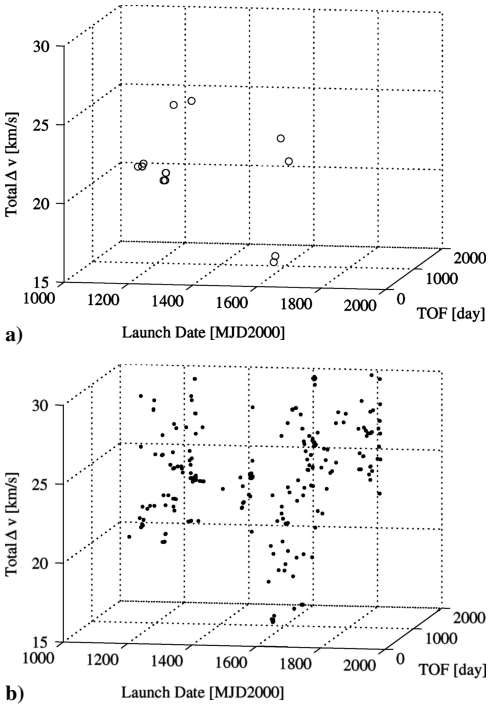

Fig. 5 Distribution of local minima: a) without DSM and b) with DSM.

swing-by is delayed. As can be seen, due to the periodicity in η, the search domain is generally multimodal, but an increase of ε causes a significant increase in multimodality.

This behavior is similar for both the mentioned choices of the reference vector $\boldsymbol{n}_i$, although it has been noticed that choosing the normal direction to the incoming velocity in the xy plane leads to a more irregular solution space. Moreover this latter choice would make the discrimination of those flybys that maximize the energy gain, from those that maximize energy loss, quite difficult. In this respect, the former choice is much more intuitive because all flybys maximizing the energy gain have $\eta \in [\pi/2, 3/2\pi]$, whereas those which maximizing the energy loss have $\eta \in [-\pi/2, \pi/2]$. For this reason, this choice has been adopted in the remainder of this work.

The consequences of the introduction of a DSM along a multiple GA trajectory can be illustrated by the following example of a transfer from the Earth to Jupiter via a swing-by of Venus. Two cases are analyzed: In the first case, the swing-by model in Fig. 3b is used and a corrective DSM is performed after the swing-by, whereas in the second case, a simple velocity matching at the swing-by planet is performed (no DSM).

Position and velocity of the three planets are functions of the departure time t_0 and of the time of flight to Venus and to Jupiter T_1 and T_2. The impulsive maneuvers necessary to accomplish these transfers are $\Delta \boldsymbol{v}_1$to leave the Earth, $\Delta \boldsymbol{v}_s$, which is either the required correction to match the outgoing velocity at the flyby in the case of no DSM, or the magnitude of the DSM itself, and $\Delta \boldsymbol{v}_2$ the arrival velocity at Jupiter. The total cost of the transfer can be expressed as

$$f(t_0, T_1, h, \eta, \varepsilon, T_2) = \Delta v_1 + \Delta v_s + \Delta v_2 \tag{9}$$

with ε being fixed to zero in the case of no DSM or free to vary between the instant of the flyby and 90% of the transfer time T_2 when a DSM is included.

The analysis of cost function in Eq. (9) has been performed by taking a set of 10,000 randomly generated sample points and performing from each one a local search. The samples were generated using a Latin hypercube distribution, and the MATLAB® function, fmincon, was used for the local search setting the tolerance on optimality to $1e-6$. This approach is considered satisfactory to give a rough characterization of the solution domain.

As can be seen from the comparison of Figs. 5a and 5b, where all of the solutions with a total Δv lower than 30 km/s are shown, in the case of no DSM, there are two limited groups of local minima that are distributed over the launch dates corresponding to the synodic period of the Earth–Venus system. The situation becomes completely different in the case of a DSM performed after the swing-by of Venus. Although the globally optimal launch window is still the same, the number of opportunities for that window has increased and the distribution of the local minima is now almost continuous over the launch dates up to the epoch 1800 modified Julian date (MJD). Whereas an increase in the degrees of freedom due to the DSM could be somehow expected, less obvious is the benefit in terms of number of optimal solutions resulting from the increased complexity and multimodality of the problem.

The result of this simple test essentially shows that a simple model might not contain the required solutions, but on the other hand, a complex model could have such solutions so nested that finding them would be extremely difficult. In the following sections, we will opt for a compromise between model complexity and model fidelity, relying on a global search algorithm for the analysis of the search space. This algorithm implements a general purposes strategy and is not endowed with additional information about the specific problem under study.

III. Complete Trajectory Model and Problem Formulation

Each single subproblem, introduced and analyzed in the preceding sections, has been assembled into a complete model in which the trajectory is divided into a number of phases connecting a sequence of celestial bodies. (The full trajectory model is shown in Fig. 6.) Given a sequence of N_P planets, there exist $k = 1, \ldots, N_P - 1$ phases, each of them beginning and ending with an encounter with a planet. Each phase k is made of two conic arcs, the first ending where the second begins and having a discontinuity in the absolute heliocentric velocity at their matching point M_k. Given the transfer time T_k, relative to each phase k, and the variable $\varepsilon_\kappa = [0, 1]$, the matching point is then at $t_{\mathrm{dsk}} = t_{k-1} + \varepsilon_k T_k$. The velocity vector at infinity at departure, for the zero sphere-of-influence model, may be treated explicitly as a design parameter through the

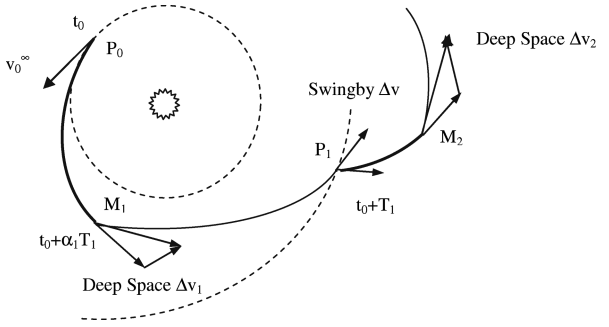

Fig. 6 Schematic of multiple GA trajectories.

following definition:

$$\boldsymbol{v}_0^{\infty} = \sqrt{C_3}(\sin\delta\cos\alpha, \sin\delta\sin\alpha, \cos\delta) \tag{10}$$

with the angles δ and α representing the declination and the right ascension of the escape asymptote, respectively. This choice allows the escape velocity and asymptote direction to be easily bound within lower and upper values while adding the possibility of having a DSM in the first arc after the launch. This is often the case when escape velocity must be fixed due to the launcher capability or to the requirement of a resonant flyby of the Earth. Alternatively it is possible to use a simplified model in which the first leg from P_0 to P_1 is a simple Lambert's arc with no DSM. In this case, the number of optimization parameters and degrees of freedom are reduced and the model is suitable for the assessment of sequences that fly directly to another planet after launch.

Once the heliocentric initial velocity, which can be the result of a flyby maneuver or the asymptotic velocity after launch, is defined for each phase k, the trajectory is analytically propagated until time $t_{\mathrm{ds}k}$. The second arc of phase k is then solved through Lambert's algorithm, from $\boldsymbol{r}_{\mathrm{ds}k}$, the Cartesian position of the DSM, to $\boldsymbol{r}_{k+1}$, the position of the target planet of phase k, for a time of flight $(1-\varepsilon_k)T_k$. Two subsequent phases are then joined together using the swing-by model given by Eqs. (5–7). The solution vector for this model can be defined as

$$\boldsymbol{y} = \left[v_0^{\infty}, \alpha, \delta, t_0, T_1, \varepsilon_1, \eta_1, h_1, \right.$$

$$\left. \ldots, T_k, \varepsilon_k, \eta_k, h_k, \ldots, T_{Np-1}, \varepsilon_{Np-1}\right]^T \tag{11}$$

where t_0 is the departure date. Now, the design of a multi-gravity-assist transfer can be transcribed into a general nonlinear programming problem, with simple box constraints, of the form

$$\min F(\boldsymbol{y}), \qquad \text{with} \qquad \boldsymbol{y} \in D \tag{12}$$

One of the appealing aspects of this formulation is its solvability through a general global search method for box constrained problems, such as evolutionary algorithms (EA).[24] Depending on the kind of problem under study, the objective function can be defined as

$$F(\boldsymbol{y}) = \left\|\boldsymbol{v}_0^{\infty}\right\| + \sum_{k=1}^{N_p-1} \|\Delta\boldsymbol{v}_k\| + \left\|\boldsymbol{v}_{Np}^{\infty}\right\| \tag{13}$$

or if the launch velocity is fixed to a given maximum value, as

$$F(\boldsymbol{y}) = \sum_{k=1}^{N_p-1} \|\Delta\boldsymbol{v}_k\| + \left\|\boldsymbol{v}_{Np}^{\infty}\right\| \tag{14}$$

Once the problem in Eq. (12) is formulated for a given sequence of GA bodies, a search over a large range of launch dates, encounter times, and GA characteristics can be started, to locate the best GA trajectory to reach a target planet. Furthermore, if the sequence of planetary encounters is left free, the problem in Eq. (12) has to be extended to handle mixed integer-real parameters (MINLP problem). In this case, fixing the maximum number of encounters the solution vector becomes

$$\boldsymbol{y} = \left[p_{1,}, \ldots, p_k, \ldots, p_{N_p-1}, v_0^{\infty}, \alpha, \delta, t_0, T_1, \varepsilon_1, \eta_1, h_1, \right.$$

$$\left. \ldots, T_k, \varepsilon_k, \eta_k, h_k, \ldots, T_{Np-1}, \varepsilon_{Np-1}\right]^T \tag{15}$$

where p_k is the identification reference number of planet kth or of any other object available in the database with the required orbital elements. In this case, the integer part of the problem represents a combinatorial problem in which only few optimal sequences are of interest. Note that if all of the sequences of any length are of interest, this is not a clever way of formulating the problem. A better approach would be to decouple the combinatorial part from the real-value part. For the same reason, we have not inserted the length of the sequence into the vector $\boldsymbol{y}$ because this parameter belongs to a one-dimensional limited and countable set containing just a limited number of interesting elements.

IV. Global Search Through a Hybrid EA

A. Search and Optimization Issues

If N_P is the number of planets in the sequence under investigation, then the number of design parameters increases as $n = 4N_p - 2$, with a typical number of design parameters ranging from 18 to 22 in the case of a mission with two or three flybys. When the implementation of a systematic search method is supposed, one option could be to discretize the search domain and evaluate each possible solution. If only two samples are taken for each variable in the case of a transfer with four flybys, such as the Cassini trajectory, at least $2^{22} = 4{,}194{,}304$ evaluations of the objective function would be necessary.

On the other hand, if we require to this simple systematic search algorithm to be complete, that is, to guarantee convergence to a globally optimal solution, for a block-box real-valued problem, an infinite number of samples densely distributed over the whole solution space would be required. Note that completeness of the search and exhaustiveness of the search, in this case, coincide because the algorithm does not have simply to find a solution but has to prove that there are no other better solutions. This makes a complete search practically impossible without any additional information on the landscape of the search space.

If completeness is dropped, in practice, then the aim could be to find a good set of solutions in a realistic computational time, while retaining the theoretical completeness of the search algorithm. To this aim, we could use a stochastic sampling algorithm based on some efficient heuristics that drives the sampling procedure, such as EA.

Because the probability of finding a solution is dependent on the density of samples in a given region, it would be desirable to prune the unpromising areas of the solution space. This is achieved through a proper blending of an evolutionary-based algorithm with a systematic branching strategy, as will be described in the following sections.

B. Evolutionary-Branching Principle

Evolutionary branching (EB) is a hybrid deterministic-stochastic approach to the solution and characterization of constrained and unconstrained multimodal, multivariate nonlinear programming problems with mixed integer-real variables and discontinuous quantities. The EB approach is based on the following principal ideas:

1) An EA is used to explore the solution space D, then a branching scheme, dependent on the findings of the evolutionary step, is used to partition the solution domain into subdomains D_l. If necessary, on each D_l a new evolutionary search is performed and the process is repeated until a number of good minima and, eventually, the global one are found (practical convergence) or the entire domain has been partitioned into infinitesimal subdomains (theoretical convergence).

2) The search is performed by a population of individuals $\boldsymbol{y}$, each one represented by a string of length n, containing in the first m components integer values and in the remaining n–m components real values. A hypercube $\boldsymbol{S}$ enclosing a region of the solution space surrounding each individual is then associated to $\boldsymbol{y}$. The solution space

is explored locally by acquiring information about the landscape within each region $\boldsymbol{S}$ and globally by a portion of the population, which is continuously regenerated.

3) Each individual can communicate its findings to the others to evolve the entire population toward a better status.

4) During the evolutionary step, a discoveries–resources balance is maintained: A level of resources is associated to each individual and is reduced or increased depending on the number of good findings of the individual.

This particular hybridization of EAs is motivated by the fact that common EA need to be run several times on this problem to provide reliable results. The deterministic step is then intended to reduce the search space at every new run. A further improvement over standard EA has been achieved by an increase of the local search capabilities of each individual. This was obtained by the introduction of a novel mechanism, called perception, described next. A comparison of this approach with known global optimizers is outside the scope of this paper and may be found in Vasile[20] and Di Lizia and Radice.[21]

C. Environment Perception

Each region $\boldsymbol{S}$ is evaluated using a mechanism called perception. This operator samples the environment to improve the status of the individuals. A new region $\boldsymbol{S}$ is then associated to the best discovered value, resulting in a migration of the individual toward a place where better resources are expected. For this reason, each hypercube $\boldsymbol{S}$ is here called migration region. The set of samples in $\boldsymbol{S}$ is generated with the following procedure: A first sample $\boldsymbol{y}^{(1)}$ is generated, by mutation of $\boldsymbol{y}$ (where mutation operators are taken from standard real-valued EAs sampling mechanisms[24]), then a linear extrapolation is performed. Extrapolation generates a new sample $\boldsymbol{y}^{(2)}$on the side of the best one between $\boldsymbol{y}^{(1)}$ and $\boldsymbol{y}$ as follows:

$$\boldsymbol{y}^{(2)} = \nu\left(\boldsymbol{y}^{(1)} - \boldsymbol{y}\right) + \boldsymbol{y}^{(1)} \tag{16}$$

where $\boldsymbol{y}^{(1)}$ is here assumed to be better than $\boldsymbol{y}$ and ν is a random number taken from a uniform distribution. The two resulting individuals, $\boldsymbol{y}^{(1)}$ and $\boldsymbol{y}^{(2)}$, and the parent $\boldsymbol{y}$ are then used to generate a third individual by using second-order interpolation mating. If $\boldsymbol{p}$ is the vector difference between $\boldsymbol{y}$ and $\boldsymbol{y}^{(2)}$ and f, $f^{(1)}$, and $f^{(2)}$ are the fitness values for the three individuals $\boldsymbol{y}$, $\boldsymbol{y}^{(1)}$, and $\boldsymbol{y}^{(2)}$, respectively, then second-order interpolation mating generates an individual building a one-dimensional model of the fitness function and taking as a new individual the minimum of the result

$$\boldsymbol{y}^{(3)} = \boldsymbol{y} + \boldsymbol{p}\chi_{\min} \tag{17}$$

$$f_{\min} = a\left(\boldsymbol{y}, \boldsymbol{y}^{(1)}, \boldsymbol{y}^{(2)}\right)\chi_{\min}^2 + b\left(\boldsymbol{y}, \boldsymbol{y}^{(1)}, \boldsymbol{y}^{(2)}\right)\chi_{\min} + f(\boldsymbol{y}) \tag{18}$$

The procedure is repeated until either an improvement of $\boldsymbol{y}$ is found or a number of samples equal to the level of resources has been generated. The level of resources is increased by one unit if an improvement occurs and is decreased by one unit if nothing is found. The upper limit has been fixed to the number of coordinates and the lower limit set to 1.

The contraction or expansion of each region $\boldsymbol{S}$ is regulated through a parameter ρ, called migration radius, which depends on the findings of the perception mechanism. The migration radius is defined as the ratio between the value of the distance from the boundary $\boldsymbol{b}_j$ of the migration region of the jth individual and the value of the distance from the corresponding boundary $\boldsymbol{b}$ of the domain D:

$$\rho_j = \frac{b_{i,j} - y_{i,j}}{b_i - y_{i,j}} \tag{19}$$

If none of the samples in $\boldsymbol{S}$ is better than $\boldsymbol{y}$, the radius is reduced according to

$$\rho_j = \begin{cases} \max([1e-8, \delta y_{\min}]), & \text{if} \quad \delta y_{\min} \geq \varepsilon\rho_j \\ \varepsilon\rho_j, & \text{if} \quad \delta y_{\min} < \varepsilon\rho_j \end{cases} \tag{20}$$

where ε has been set to 0.5 and $\delta y_{\min}$ is the distance of the best sample $\boldsymbol{y}^*$, among the ones in the migration region, from the $\boldsymbol{y}_j$, normalized with respect to the dimensions of the migration region:

$$\delta y_{\min} = \sqrt{\sum_{i=1}^{n}\left(\frac{y_i^* - y_{i,j}}{S_{i,j}}\right)^2} \tag{21}$$

where, for the jth individual and for dimension i, here $S_{i,j}$ is the difference between the value of the upper bound and of the lower bound and the summation is over nonzero dimensions. Now, if from generation k to generation $k+1$ the differential improvement Δf_j, that is, the difference between the function f_j at generation k minus f_j at generation $k+1$, increases, the migration radius is recomputed according to the prediction

$$\rho_j^{(k+1)} = \rho_j^{(k)}\theta\log(e - 1 + j) \tag{22}$$

where $\theta = 2$ in this implementation.

D. Communication Mechanisms

At the end of a full evolution step, those individuals that have improved their status are inserted in a communication list and exchange information with an equal number of randomly selected individuals from the entire population. The individuals can communicate through a simple exchange of their components, the linear extrapolation in Eq. (16), or through a linear interpolation operator given by

$$\boldsymbol{y}^{(2)} = \nu\left(\boldsymbol{y}^{(1)} - \boldsymbol{y}\right) + \boldsymbol{y} \tag{23}$$

The interpolation operator is used also to prevent crowding of more than one individual in the basin of attraction of the same solution: If the reciprocal distance among two or more individuals falls down below a given threshold, the worst one is mated with the boundaries of the subdomain D_l, thus, projecting the individual into a random point within D_l, according to the following relation:

$$y_i^{(1)} = \nu b_i + (1 - \nu)y_i \tag{24}$$

E. Ranking

At each evolutionary step, the entire population of n_{pop} individuals is ranked from the best to the worst and the best n_e individuals are allowed to use the perception mechanism while the others are either hibernated, that is, no operator is applied, or mutated. The probability of being mutated or hibernated depends on their ranking: the lower the rank position is, the higher the chance to be mutated.

F. Branching Step

Even though the evolutionary step can find several optima and eventually the global one, convergence is not guaranteed because of the stochastic nature of the process. Therefore, a systematic decomposition of the solution space is performed on the basis of the output of the EA.

The initial domain D is recursively partitioned generating a number of smaller and smaller subdomains D_l. The partitioning, or branching, process selects the worst individual $\boldsymbol{y}_{\text{worst}}$, found by the evolutionary step within D_l (with $D_0 = D$), and decomposes D_l into $2n$ subdomains, or nodes, by cutting the coordinates along the components of $\boldsymbol{y}_{\text{worst}}$. (A safeguard mechanism prevents cuts too close to a boundary by moving the cutting point to the middle of the interval.)

For each node, the ratio between the relative number of individuals and the relative volume is computed, and the resulting quantity defines how necessary a further exploration of the node is:

$$\varpi_{Dq} = \frac{\sum_{D_q} j}{\sum_{D_l} j} \Bigg/ \sqrt[n]{\frac{V_{D_q}}{V_{D_l}}}, \qquad q = 1, \ldots, 2n \tag{25}$$

where the volumes V_{Dq} and V_{Dl} are computed taking only edges with a nonzero dimension. This quantity is then added to a fitness

φ_{Dq} defined as

$$\varphi_{Dq} = \begin{cases} \dfrac{(1/J)\sum_{j=1}^{J} f_j - f_{\text{best}}}{f_{\text{worst}} - f_{\text{best}}} & \text{if} \quad J \neq 0 \\ 1 & \text{otherwise} \end{cases} \tag{26}$$

where J is the number of individuals in domain D_q, whereas f_{best} and f_{worst} are the best fitness values in the whole population and the worst fitness value in the whole population, respectively. The node is then qualified by the quantity

$$\psi_{Dq} = \sigma \varpi_{Dq} + (1 - \sigma)\varphi_{Dq} \tag{27}$$

where σ is the weighting factor that weights how reliable the result coming from the evolution step is considered. If σ is 0, only the nodes with low fitness are explored because the EA is considered reliable enough to explore exhaustively the domain D_l without leaving any region unexplored. On the other hand, if σ is 1, the result from the EA is considered to be not reliable due to a premature convergence or to a poor exploration of the solution space.

Among all $2n$ nodes, only the best pair according to quantity in Eq. (27) is selected; then, to avoid the rediscovery of already found minima, a second cut is performed at the best converged individual $\boldsymbol{y}_{\text{best}}$ and two additional nodes are selected. Therefore, at end of the branching step, the subdomain D_l has been divided into three new subdomains. These nodes are added to the list of all of the L potentially interesting subdomain such that

$$D = \bigcup_{l=1}^{L} D_l \tag{28}$$

Once the list is ranked from the best to the worst, according to Eq. (27), the best node is selected for further exploration.

G. Stopping Criteria

In this work, three stopping criteria are used: the maximum number of function evaluations, the number of times subdomains have been branched without improvement, or branching level, and the convergence of the best individual (only for the evolutionary step). All of them are based on some heuristics and not on any rigorous proof of global convergence. Note, however, that the branching scheme is devised to asympthotically partition the whole domain D into infinitesimal subdomains and, therefore, to converge globally. Finally, solution accuracy is enhanced starting a local search with a sequential quadratic programming (SQP) algorithm from each one of the best solutions found by the EB algorithm. Note, however, that, in the cases of a direct transfer or single flyby trajectory, the value of the solution obtained by EB scheme, within a typical number of function evaluations, could not be improved further by the SQP algorithm because local convergence had already been achieved. Pseudocode for the branching algorithm is given as follows:

```
Set L = 1, l = 0
Initialize D_l

Do While stopping.criteria = false

   Run Evolution on D_l

   Select y_worst and y_best
   Branch D_l = ∪_{q=1}^{2n} D_q
   Select D_q,      q = 1, ..., 3
   Add D_q to subdomain list
   L = L + 3
   l = 1, ..., L
   Select D_l

End Do
```

Pseudocode for the EA is as follows:

```
Initialize y
Do While stopping.evolution = false
   Apply Communication
   Rank y
   Select best n_e individuals
   Apply mutation to n_pop-n_e individuals
   For j = 1 to n_e
      Do while s < s_max
         Mutate y_j
         Apply Linear Extrapolation
         Apply Second-order Interpolation
         s = s + 1
      End Do
      Update ρ_j
   End For
   Rank y
   Update resources s
   Create communication list
End Do
```

V. Case Studies

The methodology presented in the preceding sections is at the core of a preliminary design tool, implemented in MATLAB, called Interplanetary Mission Analysis Global Optimization (IMAGO). IMAGO combines the described trajectory model with the EB algorithm called EPIC. In the following sections, the tool is tested on a number of difficult cases: the design of multiple transfer options to Jupiter in the case of free flybys sequence, the design of the Cassini trajectory, the design of a near-Earth orbit interception mission, and finally the design of the Rosetta mission. All of the tests have been performed on a 2-GHz Intel Centrino processor with Windows XP.

A. Missions to Jupiter

This first case study requires the design of optimal free-sequence transfers to Jupiter: Only the arrival planet, the departure planet, and the maximum number of swing-bys have been defined, whereas the sequence of planetary encounters is left free. Table 1 shows the solution domain for the Earth–Jupiter transfer problem, where the pericenter altitudes $\bar{h}_k$ are normalized with respect to the planet mean radius.

The number of possible encounters has been limited to three because a larger number would excessively increase the total transfer time while adding little benefits. The launch date can vary between 2010 and 2020 to look for multiple alternative launch opportunities. The range of possible planets goes from Venus (number 2) to Mars (number 4) for the first two gravity maneuvers and from Venus to Jupiter (number 5) for the third one. It can be seen that the upper bound on the last swing-by allows flying directly to Jupiter and, thus, to investigate solutions with a reduced number of gravity maneuvers. For this first test case, a population of 40 individuals has been used with $n_e = 20$ individuals and 4 levels of branching. This resulted in 8 h of computing time and about 1000 solutions with different combinations of planets and launch dates. For a more extensive search, the algorithm was run three times and we show in Table 2 some interesting solutions that represent a valid alternative to the trajectories reported in the work of Petropoulos et al.[13]

Table 1 Solution domain for Earth–Jupiter problem

Bounds	p_1	p_2	p_3	t_0, MJD 2000	T_1, days	$\bar{h}_1$	T_2, days	ε_1	$\bar{h}_2$	T_3, days	ε_2	$\bar{h}_3$	T_4, days	ε_3
U_b	2	2	2	3650	80	0.04	80	0.01	0.04	80	0.01	0.04	600	0.01
L_b	4	4	5	7300	400	14	800	0.9	14	800	0.90	14	2000	0.90

Table 2 Summary of interesting options for transfer to Jupiter

Sequence	Launch date	v_0^∞, km/s	Δv, km/s[a]	Time of flight, days	Arrival v^∞, km/s
EVEEJ	17 Aug. 2010	2.90	2.103	1896	5.640
EVEEJ	1 April 2012	3.26	0.0	2706	6.450
EVEEJ	27 Oct. 2013	3.69	0.134	2082	5.798
EVEEJ	26 Oct. 2013	3.68	0.174	2005	6.270
EVVEJ	28 Oct. 2013	3.87	0.620	2404	6.305
EMMJ	20 March 2014	3.31	3.100	2243	4.640
EVEMJ	20 Jan. 2017	3.68	0.648 (2) + 0.544 (3)	3112	6.639
EVEEJ	14 March 2020	3.09	0.109	2519	6.210
EVEEJ	20 March 2020	3.01	0.546	2740	5.564
EVEEJ	23 March 2020	2.99	0.125	2545	5.575
EVEEJ	26 Oct. 2021	3.34	0.223 (2) + 1.327 (3)	1979	5.609
EVVEJ	11 Dec. 2021	4.22	0.183	2577	6.102
EVEEJ	1 June 2023	3.30	0.0	2498	5.746
EVEEJ	2 July 2026	3.29	0.853	2133	6.359
EVEJ	18 Oct. 2029	3.13	1.668	1473	6.080

[a]Parenthetical numbers indicate the flyby number after which a maneuver occurs.

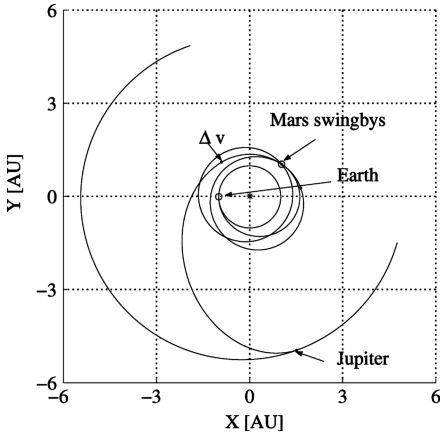

Fig. 7 Projection into ecliptic plane of the sequence EMMJ.

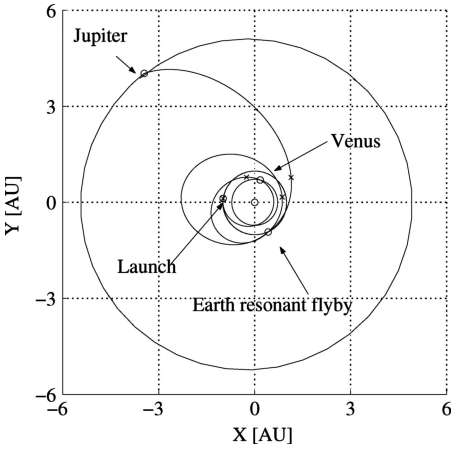

Fig. 8 Solution for EVEEJ sequence for 2009 launch.

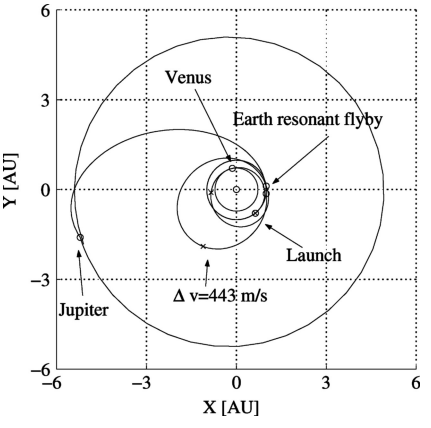

Fig. 9 Solution for EVEEJ sequence for 2010 launch.

Note that the tool was able to identify the typical optimal sequences for a mission to Jupiter, such as Earth–Venus–Venus–Earth–Jupiter (EVVEJ) or EVEEJ and to provide for these sequences some interesting solutions in terms of escape and arrival velocity. Furthermore, it is interesting to underline the Mars resonant solution: Although no particular prescription on the kind of solution was set, and additionally no particular model is implemented to generate solutions that exploit resonant swing-bys, the Earth–Mars–Mars–Jupiter (EMMJ) transfer (Fig. 7) was found as a result of the search step. It is an interesting solution because it presents an unusual possibility for a transfer to Jupiter that, although requiring a large deep space correction, could be effectively implemented through a low-thrust propulsion system.

To extend the validation of the tool, the sequence EVEEJ has been further investigated in the years 2009 and 2010 and compared to some solutions found in the literature.[13,25] Transfer time to Venus and to the first Earth flyby can vary between 70 and 550 days, whereas the transfer time to the second Earth flyby can be as long as 800 days, thus, allowing the possibility of having a two years resonant orbit after the first flyby. Last, the transfer time to Jupiter can vary between 400 and 1600 days. A DSM can be applied up to 90% of the transfer time after each flyby, although the maximum altitude of the swing-by maneuver is bounded below by 300 km for Venus and by 1000 km for Earth.

For this test, which has a fixed sequence and smaller bounds on the launch date, it was sufficient to use only the evolutionary step. A population of 40 individuals has been evolved for a maximum number of 200,000 function evaluations. The parameter n_e has been set equal to 25, thus, favoring convergence rather than exploration. Although not exploiting the whole investigation capability offered by the search algorithm, as can be seen in Table 3, there is a good agreement between the solution computed by IMAGO and the reference solution. In Figs. 8 and 9 two examples for the sequence EVEEJ for the 2009 and 2010 launch dates are shown, whereas Tables 3 and 4 show three and two solutions found for the 2009 and 2010 launch date and a comparison with the best solutions found by Petropoulos et al.[13] for the same launch year, respectively.

Note that for both launch options, IMAGO was able to locate, in approximately 20 min of computational time, within the launch window some solutions already known in the literature. However, an improvement over the reference solution is shown in terms of both total Δv and transfer time.

Table 3 Summary and comparison of different options for 2009 launch window

Solutions	Launch date	v_0^∞, km/s	Δv, km/s	Time of flight, days	Arrival v^∞, km/s
2009 ESOC[a]	4–24 March 2009	4.08–4.38	0.05	2046–2096	5.87–5.99
Petropoulos et al.[13]	21 Jan. 2009	3.68	0.00	2299	5.50
IMAGO1	15 March 2009	4.04	0.00	2067	6.00
IMAGO2	17 March 2009	4.09	0.00	2209	5.55
IMAGO3	31 Jan. 2009	3.69	0.03	2238	5.59

[a]European Space Operations Center.

Table 4 Summary and comparison of different options for 2010 launch window

Solutions	Launch date	v_0^∞, km/s	Δv, km/s	Time of flight, days	Arrival v^∞, km/s
2010 ESOC	1 July–31 Aug. 2010	2.81–2.97	0.500	2379–2426	5.92–6.33
Petropoulos et al.[13]	21 July 2010	2.94	0.360	2409	6.21
IMAGO1	4 Aug. 2010	2.73	0.380	2387	5.53
IMAGO2	3 Aug. 2010	2.91	0.538	2424	5.80

Table 5 Bounds on design parameters for Cassini trajectory

Bounds	T_1, days	T_2, days	T_3, days	T_4, days	T_5, days	$\bar{h}_1$	$\bar{h}_2$	$\bar{h}_3$	$\bar{h}_4$
L_b	100	100	30	400	800	0.05	0.05	0.15	0.7
U_b	400	500	300	1600	2200	5	5	5.5	290

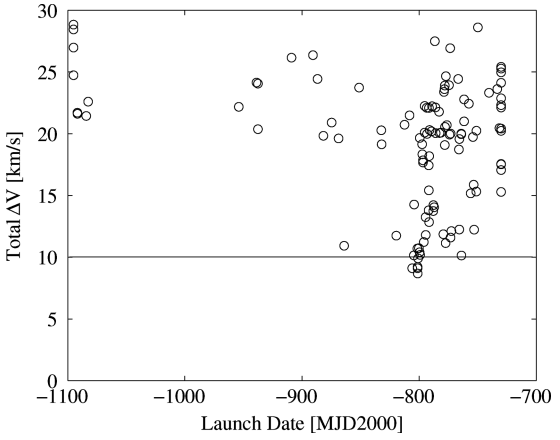

Fig. 10 Distribution of optimal solutions found for 1997 launch for Cassini.

B. Cassini Trajectory Design

The design of the Cassini trajectory is an interesting test case because it is one of the most complex multiple GA (MGA) trajectories designed for a mission to an outer planet. Furthermore, the arrival velocity must be kept sufficiently low to allow the insertion into the Saturn planetary system, and the high mass budget of the spacecraft limits the launch hyperbolic escape velocity provided by the launcher, below 4 km/s. The launch date investigated is 1997, and the other bounds on the design parameters are reported in Table 5: a DSM can occur up to 90% of the transfer time to each planet.

As can be seen in Table 5, the bounds on the transfer time are quite broad because in every preliminary design phase there is a lack of preliminary information on possible good options, and every possibility should be investigated. This test case, thus, reproduces the typical preliminary design conditions when little information is available. The preliminary design is then initiated by looking for solutions minimizing the function in Eq. (13). For this test, a population of 40 individuals has been used with a parameter n_e equal to 25 and two levels of branching. The total number of function evaluations was a little bit more than 800,000, with a final number of around 200 generated solutions. Figure 10 shows all of the local minima that have been found in the search domain: Most of them are distributed around the date −800 MJD, which is the optimal launch window that collects all of the solutions with a total Δv of approximately 10 km/s (the total Δv of Cassini). Figure 11 shows the EVVE part of the transfer with the Venus–targeting Δv maneuver.

Table 6 Summary and comparison of different options for Cassini

Mission parameter	Cassini	Solution IMAGO1	Solution IMAGO2
Launch date	15 Oct. 1997	20 Oct. 1997	17 Oct. 1997
v_0^∞, km/s	3.93	4.04	4.03
EV TOF,[a] days	194	191	191
VV DSM, km/s	0.471	0.432	0.414
VV TOF, days	425	421	420
VE DSM, km/s	0	0	0
VE TOF days	54	53	53
EJ DSM km/s	0	0.132	0
EJ TOF days	499	493	540
JS DSM km/s	0.376	0	0
JS TOF days	1267	1216	1656
Total Δv km/s	10.14	10.18	9.06

[a]Time of flight.

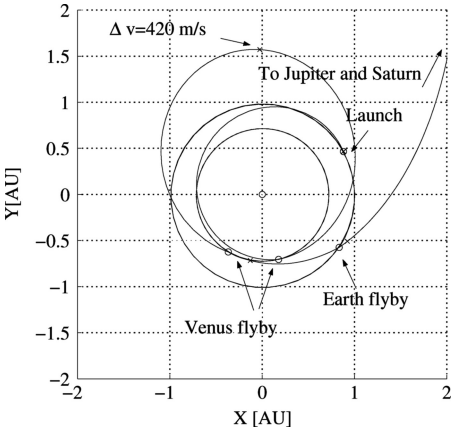

Fig. 11 Close view of sequence of flybys of inner planets for Cassini.

In Table 6, the reference solution for the Cassini mission and two of the best solutions found by IMAGO have been compared. Note the similarity of the first solution with the reference solution in terms of both launch dates and total Δv, whereas the second solution presents an interesting saving in the arrival velocity at the expense of a higher transfer time.

Table 7 Bounds on the design parameters for the mission to asteroid (10302)-1989ML

Bounds	t_0	ε_1	$\bar{h}_1$	T_1, days	ε_2	$\bar{h}_2$	T_2, days	ε_3	T_3, days
U_b	4015	0.01	0.1	80	0.01	0.1	80	0.01	600
L_b	5100	0.90	14	400	0.90	14	800	0.90	2000

Table 8 Summary of different solutions for mission to asteroid (10302)-1989ML

	Solution				
Mission parameter	IMAGO1	IMAGO2	IMAGO3	IMAGO4	IMAGO5
Launch date	5 Jan. 2011	1 Jan. 2011	3 Nov. 2011	19 Oct. 2011	26 March 2011
v_0^∞, km/s	3.99	3.59	3.85	3.64	3.8
EE DSM, km/s	0	0	0	0	0
EE TOF, days	182	182	179	178	365
EV DSM, km/s	0	0.314	0	0.341	0.327
EV TOF, days	641	726	168	179	191
E–asteroid DSM, km/s	0	0	0.389	0	0
E–asteroid TOF, days	603	791	478	471	469
Arrival v^∞, km/s	13.08	13.15	16.81	16.34	15.77

As further verification, the same problem with the same model has been solved with a simple multistart technique: 100 samples of each parameter have been taken with a Latin hypercube distribution, and the best three samples have been optimized with a local procedure using the MATLAB function fmincon. The procedure has been repeated for 30 independent runs for a total of about 1,600,000 function evaluations. Although the overall number of function evaluations is twice that of IMAGO, the total number of good solutions is lower. Furthermore, although this procedure was run several times, the best solutions obtained with the multistart approach were worse than the ones produced by IMAGO. This proves that a simple random approach with a simple heuristics cannot efficiently solve this problem. This was proven to be even truer for problems of higher complexity or for an extended launch window.

C. Missions to Asteroid (10302)-1989ML

Missions to asteroids have been gaining increasing interest over the past few years, both for scientific reasons and for hazard mitigation. In particular, the mission Don Quijote,[26] currently under study in Europe, is planning to fly two twin spacecraft to asteroid (10302)-1989ML to perform scientific investigations with one satellite while the other impacts the asteroid at a high speed (greater than 10 km/s). The trajectory of the impacting spacecraft has been taken as the reference solution for this analysis.

The search was performed over a launch window in 2011, and only the solutions with an arrival velocity greater than 10 km/s have been retained. In this case, only the evolutionary step was used with a population of 30 individuals and a maximum number of 100,000 function evaluations.

The reference solution proposes a first Earth swing-by after 180 days to separate the two spacecraft that have been launched together; therefore, the selected sequence is EEV–asteroid. Here the bounds on the EE transfer orbit (design parameters in Table 7) can range from 80 to 400 days, hence, allowing the investigation of other possible options and particularly a one-to-one resonant flyby with the Earth (Table 8). Transfers with a 180-day Earth-to-Earth flyby are the most recurrent solutions and can be classified into two groups: short-period EV, V–asteroid transfers (Fig. 12) and long-period EV, V–asteroid transfers (Fig. 13). The latter have a bound orbit before the encounter with Venus and a second bound orbit before the impact.

D. Rosetta Trajectory Design

The preliminary design of the Rosetta mission represents an interesting test case for two different reasons. First, the trajectory rendezvouses with a comet on an elliptical orbit, after a number of swing-bys and DSMs. Second, it is an interesting example of the demand for a quick investigation of different backup options. The Rosetta mission, originally designed to rendezvous with comet

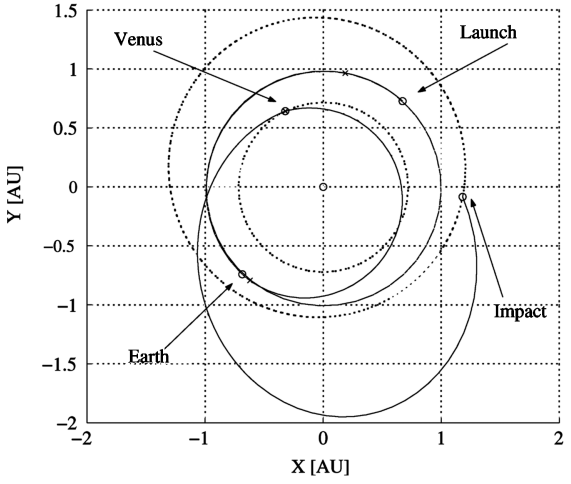

Fig. 12 Solution IMAGO3: projection into the ecliptic plane.

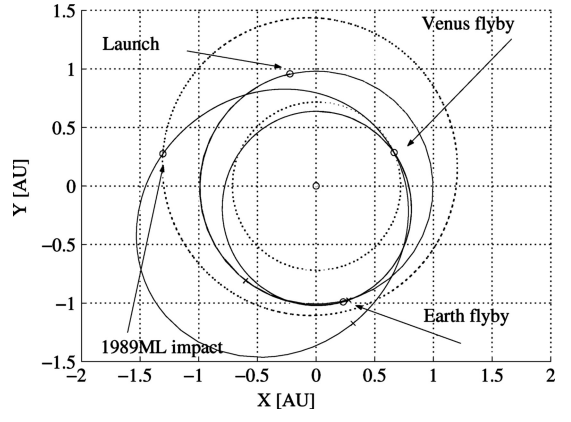

Fig. 13 Solution IMAGO1: projection into the ecliptic plane.

Wirtanen, was not launched in January 2003 due to technical problems with Ariane-5 and was completely redesigned for a new target and set to launch in 2004. This required a new investigation and characterization of all of the trajectory opportunities, along with the definition of a new target. For this reason, this test case has been approached supposing very little knowledge on the structure of the solutions in terms of launch date and deep space corrections. The sequence has been chosen to be EEMEE–comet, which is the solution adopted for the new Rosetta mission.[27]

Table 9 Bounds on design parameters for Rosetta trajectory

Bounds	t_0, MJD 2000	T_1, days	ε_1	$\bar{h}_1$	T_2, days	ε_2	$\bar{h}_2$	T_3, days	ε_3	$\bar{h}_3$	T_4, days	ε_4	$\bar{h}_4$	ε_5	T_5, days
U_b	1460	300	0	0.06	150	0	0.06	150	0	0.06	300	0	0.06	0	700
L_b	1825	400	0.9	9	800	0.9	9	800	0.9	9	800	0.9	9	0.9	1850

Table 10 Summary of options for Rosetta mission

Mission parameters	Rosetta	Solutions			
		IMAGO1	IMAGO2	IMAGO3	IMAGO4
Launch date	2 March 2004	5 March 2004	7 March 2004	27 Feb. 2004	12 March 2004
v_0^∞, km/s	3.546	3.546	3.546	3.546	3.546
EE TOF, days	367	361	363	369	370
EM TOF, days	722	722	719	721	728
ME TOF, days	261	263	263	262	256
EE TOF, days	730	729	730	730	730
E–P67 TOF, days	1650	1825	1825	1642	1640
Total Δv km/s	1.700	1.763	1.581	1.702	1.921

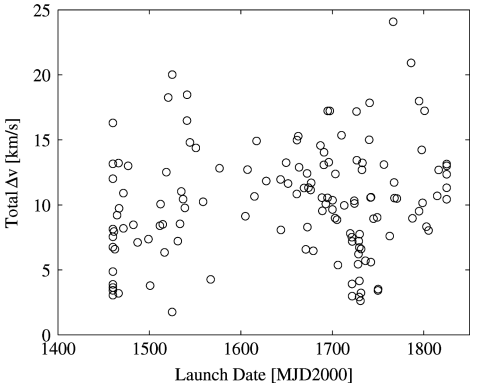

Fig. 14 Distribution of optimal solutions for Rosetta preliminary design.

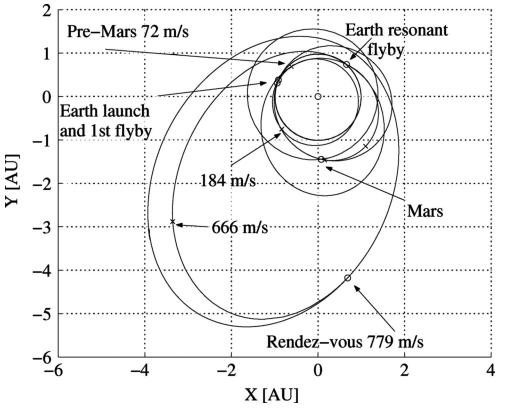

Fig. 15 Solution IMAGO3: projection into the ecliptic plane.

The design has been conducted in two different steps: As a first step, a deep investigation for a launch date in 2004, with a fixed velocity of 3.546 km/s due to the launcher capability, has been performed using the large bounds on the design parameters reported in Table 9. This is the typical situation that mission analysts would face during the preliminary design of a new mission, to assess good sequences. For this first investigation, the branching procedure was largely exploited, using two levels of branching and a maximum number of 200,000 evaluations for each evolutionary step, with a population of 40 individuals. This parameter setting results in a maximum number of some 800,000 total evaluations but yields an extensive characterization of the possible solutions and the local optima in the domains.

The results of this first extensive search are shown in Fig. 14, which shows all of the local optimal solutions located by the algorithm in a computational time of 2.5 h. Notice that there are two groups of good solutions for a launch date around 1455 MJD and a launch date around 1730 MJD, which present a total Δv of some 2–2.5 km/s and there are some other interesting options, although less crowded, for a launch around the 1530 MJD. From this information, the bounds on the search have been reduced around these groups of solutions, and a further investigation has been performed producing a large variety of good different solutions comparable with the reference one adopted for the actual mission. In this case, only the evolutionary step has been used with a maximum number of 100,000 evaluations, yielding some very good solutions, some of which are presented in Table 10, where the characteristics of the solution found are reported, whereas Fig. 15 shows the most similar solution to the reference one.

VI. Conclusions

A novel approach is presented to the automatic preliminary investigation of MGA interplanetary trajectories. An initial analysis on the relation between model completeness and solution search complexity has led to the development of a simple trajectory model sufficiently accurate for preliminary design and sufficiently complete to preserve important classes of possible solutions. The analysis performed on the domain structure of each simple subproblem, composing the whole model, although not exhaustive, has revealed a structure of the search spaces that is generally multimodal and nonconvex. These characteristics are a direct consequence of the model complexity and could be exploited to improve the search for a solution. A general global optimization approach, not problem dependent, is proposed. This novel approach blends together an evolutionary-based algorithm with a deterministic branching strategy that is used to partition the whole solution space in subdomains.

The proposed methodology has been tested on a suite of typical mission design problems of high complexity and has proved to yield good results in terms of both quality of the solutions and quantity of information they provide. In particular, the nominal Cassini trajectory has been correctly reconstructed starting from very large bounds on the design parameters and, in addition, some cheaper options in terms of total Δv have been found. The Rosetta and the asteroid impact test cases have shown how the proposed methodology is able to characterize highly complex trajectory problems yielding a good deal of different trajectory options with a total Δv comparable to the reference solutions. Finally, on the free-sequence problem, the search algorithm has performed fairly well providing some interesting families of solutions, including a few unexpected ones. Furthermore, the comparison with the Cassini and Rosetta

reference solutions, which represent the optimal trajectory actually flown, shows how the results obtained with the preliminary analysis of IMAGO are highly accurate with respect to all of the main features of the trajectory.

These results demonstrate that the proposed methodology is able to tackle effectively the complexity of MGA interplanetary transfers while avoiding being trapped in local minima, even in highly multimodal domains, where a classical optimization approach could fail. Moreover, the quality of the solutions and the low computational time make the approach appealing for the development of preliminary design tools.

Finally, the analysis performed in this paper suggests that the search for a solution can be further improved by reducing the solution space. This can be achieved by solving each subproblem in an incremental fashion and pruning part of the search domain from the early stages of development of the trajectory even for long sequences of gravity maneuvers with up to 15 or more celestial bodies as in the work of Heaton et al.[15] This is the subject of current research and will be presented in future papers.

References

[1]Labunsky, A. V., Papkov, O. V., and Sukhanov, K. G., *Multiple Gravity Assist Interplanetary Trajectories*, Earth Space Inst. Book Series, Gordon and Breach, 1998.

[2]Battin, R., *An Introduction to the Mathematics and Methods of Astrodynamics*, 1st ed., AIAA, New York, 1987, pp. 427–437.

[3]Shirley, D. L., "Mariner 10 Mission Analysis: Application of a Black Art," AIAA Paper 75-53, Jan. 1975.

[4]Kohlhase, C. E., and Penzo, P. A., "Voyager Mission Description," *Space Science Reviews, Historical Archive*, Vol. 21, No. 2, 1977, pp. 77–101.

[5]Diehl, R. E., Kaplan, D. I., and Penzo, P. A., "Satellite Tour Design for the Galileo Mission," AIAA Paper 83-101, Jan. 1983.

[6]Matson, D. L., Spilker, L. J., and Lebreton, J. P., "The Cassini Huygens Mission to the Saturnian System," *Space Science Reviews*, Vol. 104, No. 1–4, 2002, pp. 1–58.

[7]Campagnola, S., Garcia, D., Jehn, R., Corral, C., and Croon, M., "Bepi-Colombo Mercury Cornerstone Mission Analysis: Soyuz/Fregat Launch in 2012," MAO Working Paper 466, ESA/ESOC, Darmstadt, Germany, Sept. 2004.

[8]McAdams, J. V., "MESSENGER's Mission Overview and Trajectory Design," American Astronautical Society, AAS Paper 03-541, Aug. 2003.

[9]Guo, Y., and Farquhar, B. W., "Baseline Design of New Horizons Mission to Pluto and the Kuiper Belt," International Astronautical Congress, Paper IAC-04-Q.2.a.05, Oct. 2004.

[10]Vasile, M., Biesbroek, R., Summerer, L., Gálvez, A., and Kminek, G., "Options for Mission to Pluto and Beyond," 13th AAS/AIAA Space Flight Mechanics Meeting, AAS Paper 03-210, Feb. 2003.

[11]Sims, J., Staugler, A., and Longuski, J., "Trajectory Options to Pluto via Gravity Assists from Venus, Mars, and Jupiter," *Journal of Spacecraft and Rockets*, Vol. 34, No. 3, 1997, pp. 347–353.

[12]Strange, N. J., and Longuski, J. M., "Graphical Method for Gravity-Assist Trajectory Design," *Journal of Spacecraft and Rockets*, Vol. 39, No. 1, 2002, pp. 9–16.

[13]Petropoulos, A. E., Longuski, J., and Bonfiglio, E. P., "Trajectories to Jupiter via Gravity Assists from Venus, Earth, and Mars," *Journal of Spacecraft and Rockets*, Vol. 37, No. 6, 2000, pp. 776–783.

[14]Longuski, J., and Williams, S. N., "Automated Design of Gravity-Assist Trajectories to Mars and Outer Planets," *Celestial Mechanics and Dynamical Astronomy*, Vol. 52, No. 3, 1991, pp. 207–220.

[15]Heaton, A. F., Strange, N. J., Longuski, J. M., and Bonfiglio, E. P., "Automated Design of the Europa Orbiter Tour," *Journal of Spacecraft and Rockets*, Vol. 39, No. 1, 2002, pp. 23–30.

[16]Chen, K. J., Landau, D. F., McConaghy, T. T., Okutsu, M., Longuski, J. M., and Aldrin, B., "Preliminary Analysis and Design of Powered Earth-Mars Cycling Trajectories," AIAA Paper 2002-4422, Aug. 2002.

[17]Hartmann, J. W., Coverstone-Carrol, V. L., and Williams, S. N., "Optimal Interplanetary Spacecraft Trajectories via Pareto Genetic Algorithm," *Journal of the Astronautical Sciences*, Vol. 46, No. 3, 1998, pp. 267–282.

[18]Rogata, P., Di Sotto, E., Graziano, M., and Graziani, F., "Guess Value for Interplanetary Transfer Design Through Genetic Algorithms," American Astronautical Society, AAS Paper 03-140, Feb. 2003.

[19]Vasile, M., Summerer, L., and De Pascale, P., "Design of Earth-Mars Transfer Trajectories Using Evolution-Branching Technique," International Astronautical Congress, Paper IAC-03-A.7.07, Sept.–Oct. 2003.

[20]Vasile, M., "A Global Approach to Optimal Space Trajectory Design," American Astronautical Society, AAS Paper 03-141, Feb. 2003.

[21]Di Lizia, P., and Radice, G., "Advanced Global Optimization Tools for Mission Analysis and Design," Final Rept., ESA Ariadna ITT AO4532/18139/04/NL/MV,Call03/4101, Nov. 2004.

[22]Myatt, D. R., Becerra, V. M., Nasuto, S. J., and Bishop, J. M., "Advanced Global Optimization Tools for Mission Analysis and Design," Final Rept. ESA Ariadna ITT AO4532/18138/04/NL/MV,Call03/4101, Nov. 2004.

[23]Pessina, M. S., Campagnola, S., and Vasile, M., "Preliminary Analysis of Interplanetary Trajectories with Aerogravity and Gravity-Assist Manouvres," International Astronautical Congress, Paper IAC.03.P.08 Sept.–Oct. 2003.

[24]Back, T., Fogel, D., and Michalewicz, Z., *Handbook of Evolutionary Computation*, Inst. of Physics Publishing and Oxford Univ. Press, 1997.

[25]Khan, M., Campagnola, S., and Croon, M., "End to End Mission Analysis for a Low-Cost Two Spacecraft Mission to Europa," AAS/AIAA 14th Spaceflight Mechanics Meeting, AAS Paper 04-132, Feb. 2004.

[26]Gonzalez, J. A., Bellò, M., Martin-Albo, J. F., and Galvez, A., "Don Quijote: An ESA Mission for the Assessment of the NEO Threat," International Astronautical Congress, Paper IAC-04-Q.P.21, Oct. 2004.

[27]Shoenmaekers, J., and Bauske, R., "Re-Design of the Rosetta Mission for Launch in 2004," ESA and DLR, 18th International Symposium on Spaceflight Dynamics, Paper p0122, Oct. 2004.

C. Kluever
Associate Editor